A LOW INSERTION LOSS AND HIGH SELECTIVITY UWB BANDPASS FILTER USING COMPOSITE RIGHT/LEFT-HANDED MATERIAL

T.-C. Chou

Department of Electrical Engineering
National University of Tainan, Tainan, Taiwan, R.O.C.

M.-H. Tsai

Department of Electro-Optical Engineering
Kun Shan University, Tainan, Taiwan, R.O.C.

C.-Y. Chen

Department of Electrical Engineering
National University of Tainan, Tainan, Taiwan, R.O.C.

Abstract—A novel bandpass filter (BPF) based on the composite right/left-handed (CRLH) material and 0° feeding structure is proposed. With multiple unit-cells cascaded, the new section comprises the series interdigital capacitors and the shunt short-circuited stub inductors in the symmetric configuration. The circuit is designed to be unbalanced, a tunable gap between left handed and right handed modes in the $\beta - \omega$ diagram can control out of band performance. With careful design, a bandpass filter with wide rejection band can be achieved. Furthermore, by using the 0° feeding associated structure, two extra transmission zeros are created just outside the intended passband. Finally, a three cells bandpass filter has been designed and fabricated with 1.1 dB insertion loss at the center frequency of 4.2 GHz. Two transmission zeros are located at 2.95 GHz and 6.18 GHz with attenuations of -44.1 dB and -37.3 dB, respectively. Also, a wide rejection band from 5.4 to 9 GHz is obtained.

1. INTRODUCTION

Recently, introduction and applications related to left-handed metamaterial (LHM) have attracted a lot of attention. The metamaterials with negative permittivity and permeability were first proposed by Veselago in the late 1960s [1]. Simovski et al. [2] showed that the wave vector $\vec{k}$ and Poynting vector $\vec{P}$ are anti-parallel and the reversal of some basic electromagnetic phenomena such as the Snell's law, the Doppler effect, and the Vavilov-Cerenkov effect is associated with negative index of refraction. Based on the analysis of LHM, some related devices have been presented such as an electrically small dipole antenna with a shell of double negative material [3], a hybrid phase shifter using a left-handed (LH) transmission line [4], an inductively coupled two-pole bandpass filter using the zeroth-order CRLH CPW resonators [5], a simulation study leading to computer aided design (CAD) of LH-TL bandpass filters [6], a coplanar waveguide (CPW) bandpass filter (BPF) using Composite Right/Left-handed (CRLH) Zeroth-order Resonators [7], and a novel forward coupler using coupled composite right/left-handed transmission lines [8].

The composite right/left-handed (CRLH) transmission line (TL) structures using microstrip technology [9] have been implemented in the radio frequency component design When the circuit is unbalanced, the gap between left handed (LH) and right handed (RH) modes in the $\beta - \omega$ diagram can result in a rejection band and affect out of band performance. With careful design, a bandpass filter with wide rejection band can be realized Furthermore, by using the $0°$ feeding associated structure [10], two extra transmission zeros are created just outside the passband.

In this paper, an unbalanced CRLH TL based on the $0°$ feeding structure is proposed. Compared to the conventional structures, the skirt selectivity of this proposed filter is further improved. Besides, the low insertion loss and wide stop-band performances are also shown in this paper.

2. DESIGN METHODOLOGY

2.1. The CRLH TL

A symmetric CRLH TL unit cell equivalent circuit model consists of the series inductance (L_R), the series capacitance (C_L), the shunt inductance (L_L) and the shunt capacitance (C_R) is shown in Fig. 1. The transmission line matrix [ABCD] of the unit cell can be obtained
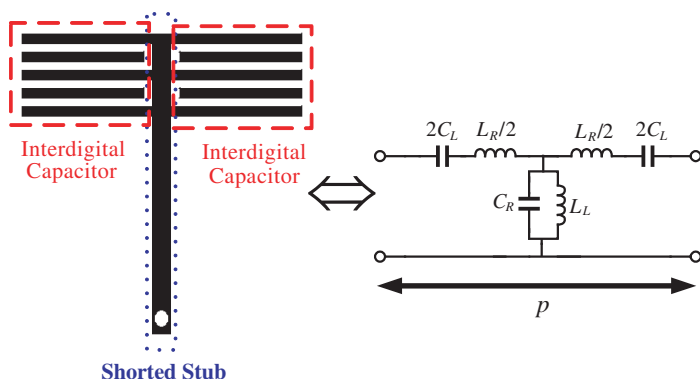
Figure 1. Layout and equivalent circuit model of a symmetric configuration CRLH TL unit cell.

as follows:

$$\begin{bmatrix} A & B \\ C & D \end{bmatrix}_R = \begin{bmatrix} 1 & \frac{j\omega L_R}{2} \\ 0 & 1 \end{bmatrix} \begin{bmatrix} 1 & 0 \\ j\omega C_R & 1 \end{bmatrix} \begin{bmatrix} 1 & \frac{j\omega L_R}{2} \\ 0 & 1 \end{bmatrix}$$

$$= \begin{bmatrix} 1 - \frac{\omega^2 L_R C_R}{2} & j\omega L_R - \frac{j\omega^3 L_R^2 C_R}{4} \\ j\omega C_R & 1 - \frac{\omega^2 L_R C_R}{2} \end{bmatrix} \quad (1)$$

$$\begin{bmatrix} A & B \\ C & D \end{bmatrix}_L = \begin{bmatrix} 1 & \frac{1}{2j\omega C_L} \\ 0 & 1 \end{bmatrix} \begin{bmatrix} 1 & 0 \\ \frac{1}{j\omega L_L} & 1 \end{bmatrix} \begin{bmatrix} 1 & \frac{1}{2j\omega C_L} \\ 0 & 1 \end{bmatrix}$$

$$= \begin{bmatrix} 1 - \frac{1}{2\omega^2 C_L L_L} & \frac{1}{j\omega C_L} - \frac{1}{4j\omega^3 L_L C_L^2} \\ \frac{1}{j\omega L_L} & 1 - \frac{1}{2\omega^2 L_L C_L} \end{bmatrix} \quad (2)$$

The S-parameters can be further derived from the transmission matrix [ABCD] and the phase shift difference of the symmetric configuration CRLH TL unit cell can be represented as [11]

$$\Delta\phi_{R,unit} = \phi(S_{21}, R) = -\arctan\left\{ \frac{\frac{\omega}{2}\left[\frac{L_R}{Z_{CR}}(1 - \frac{1}{4}\frac{\omega^2}{\omega_R^2}) + C_R Z_{CR}\right]}{1 - \frac{1}{2}\left(\frac{\omega}{\omega_R}\right)^2} \right\} \quad (3)$$

$$\Delta\phi_{L,unit} = \phi(S_{21}, L) = +\arctan\left\{ \frac{\frac{1}{2\omega}\left\{\frac{1}{Z_{CL}C_L}(1 - \frac{\omega_L^2}{4\omega^2}) + \frac{Z_{CL}}{L_L}\right\}}{1 - \frac{1}{2}\left(\frac{\omega_L}{\omega}\right)^2} \right\} \quad (4)$$

where

$$\omega_R = \frac{1}{\sqrt{L_R C_R}} \quad \omega_L = \frac{1}{\sqrt{L_L C_L}} \quad \omega = \frac{1}{\sqrt[4]{L_R C_R L_L C_L}}$$

$$Z_{CL} = \sqrt{\frac{L_L}{C_L}} \quad Z_{CR} = \sqrt{\frac{L_R}{C_R}}$$

Under the assumption of the electrical small model, the $\Delta\phi_R$ and $\Delta\phi_L$ phase shift difference resulted from a unit cell must be much smaller than $\pi/2$ [12]. Thus, the resultant phase shift difference $\Delta\phi_{CRLH}$ of the CRLH TL can be further simplified as

$$\Delta\phi_{CRLH} = \Delta\phi_{R,unit} + \Delta\phi_{L,unit} \cong - \left[\omega\sqrt{L_R C_R} - \frac{1}{\omega\sqrt{C_L L_L}} \right] \quad (5)$$

With N unit-cells cascaded, the overall length and phase shift difference become $N \times p$ and $N \times \Delta\psi$, respectively. The propagation constant can be represented in terms of L'_R, C'_R, L'_L and C'_L, which are the electrical parameters of the overall structure.

$$\beta = \omega\sqrt{L'_R C'_R} - \frac{1}{\omega\sqrt{L'_L C'_L}} \quad (6)$$

From Equation (6), the new section composed of the series interdigital capacitors and the shunt short-circuited stub inductors in the symmetric configuration can approach the characteristic of the ideal CRLH TL [9]. It is shown that the LH mode with a phase lead can be excited at low resonant frequency. Similarly, the RH mode will have a phase lag proportional to $\sqrt{L'_R C'_R}$ at high frequency.

2.2. Unbalanced CRLH TL

A symmetric CRLH TL unit cell is implemented by cascading capacitors and inductors into a conventional TL [11]. It is called a balanced structure when the series resonance ω_{se} and the shunt resonance ω_{sh} are equal ($1/\sqrt{L_R C_L} = 1/\sqrt{L_L C_R}$). On the other hand, an unbalanced structure results from the case of $\omega_{se} \neq \omega_{sh}$ ($1/\sqrt{L_R C_L} \neq 1/\sqrt{L_L C_R}$). As shown in Fig. 2, the CRLH transmission
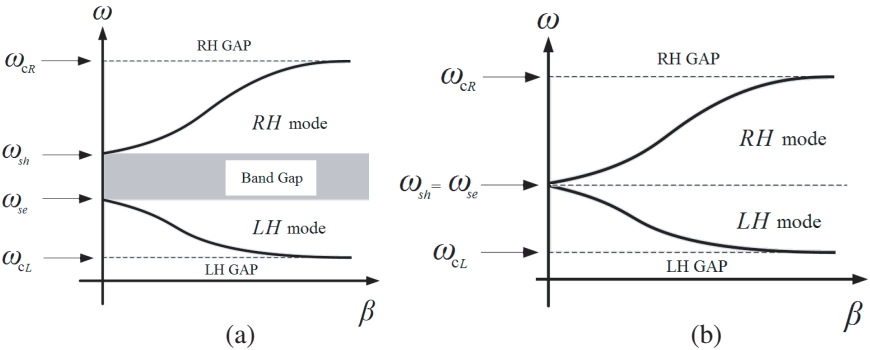

Figure 2. Typical dispersion diagram of the (a) balanced and (b) unbalance CRLH TL.

with LH behavior has the characteristics of opposite signs of a group and phase velocities in the lower frequency band. On the other hand, the CRLH transmission line with RH behavior has the same signs of the group and phase velocities in the higher frequency band.

From Equation (6), it is shown that the CRLH TL is comprised with the left handed mode at low resonant frequency and the right handed mode at high frequency. The balanced and unbalanced circuits are shown in Figs. 3(a) and (b). The former one can provide a wide passband, but it suffers from a large component size. The latter enables a rejection band to be created by controlling the gap between LH and RH modes in the $\beta - \omega$ diagram. To realize wide rejection band and compact size, such a tunable gap is utilized to inhibit out of band interference. Illustrated in Fig. 4, when a LH band is designed around the 4 GHz, a RH band can be extended to 7.8, 8.5 and 9.8 GHz. The
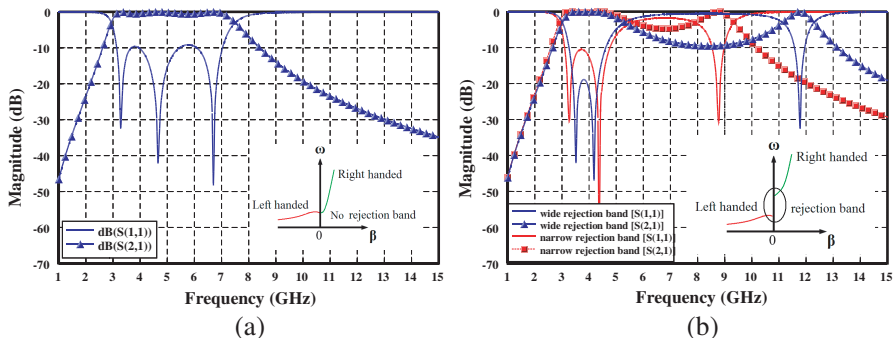

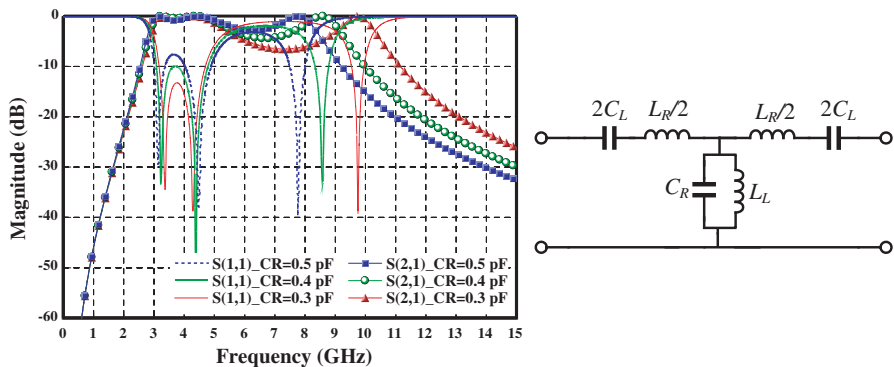**Figure 3.** (a) Balanced CRLH mode. (b) Unbalanced CRLH mode.

Figure 4. Unbalanced CRLH TL characteristics for the parameters, $C_R = 0.5$, 0.4 and 0.3 pF, $L_R = 4$ nH, $L_L = 1.9$ nH, $C_L = 0.3$ pF.
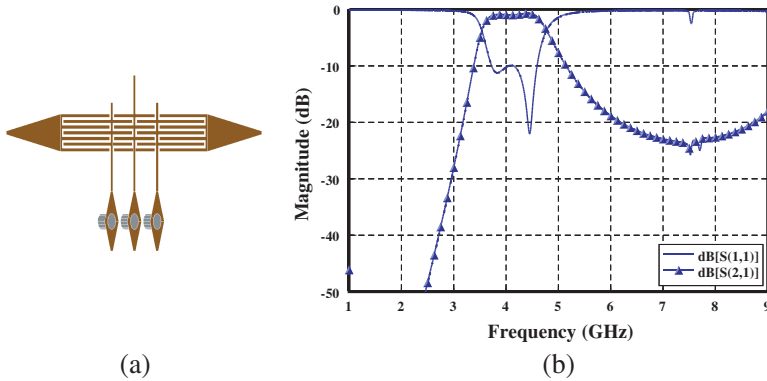
(a)   (b)

Figure 5. (a) The microstrip-BPF CRLH TL structure.   (b)
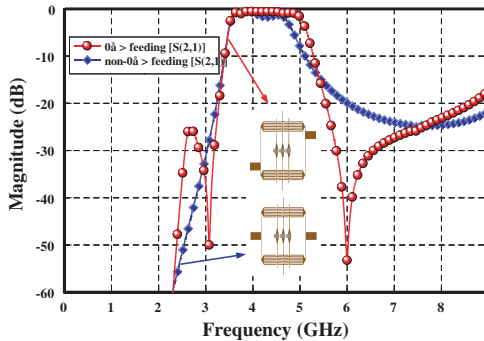Simulation results of an unbalanced CRLH TL.

Figure 6. S_{21} responses with $0°$ feed structure and non-$0°$ feed
structure.

control of the edge frequencies of the bandgap are carried out using
the different capacitance values. As shown in Figs. 5(a) and (b), the
layout of the CRLH TL for the unbalanced case has the characteristics
of flat passband performance and wide rejection band. However, the
skirt selectivity is not good enough. In references [10], both $0°$ feed
structure and non-$0°$ feed structure are introduced. The simulations for
both structures are shown in Fig. 6. It is clear that the skirt selectivity
is not good enough since no transmission zeros are created in the non-
$0°$ feed structure. With a $0°$ feed structure, two extra transmission
zeros are created just outside the passband. Besides, the open stub is
used to make impedance matching more perfect. Both without open
stub and with open stub structures are shown in Figs. 7(a) and (b). It
is obvious that the impedance matching can be improved in the case
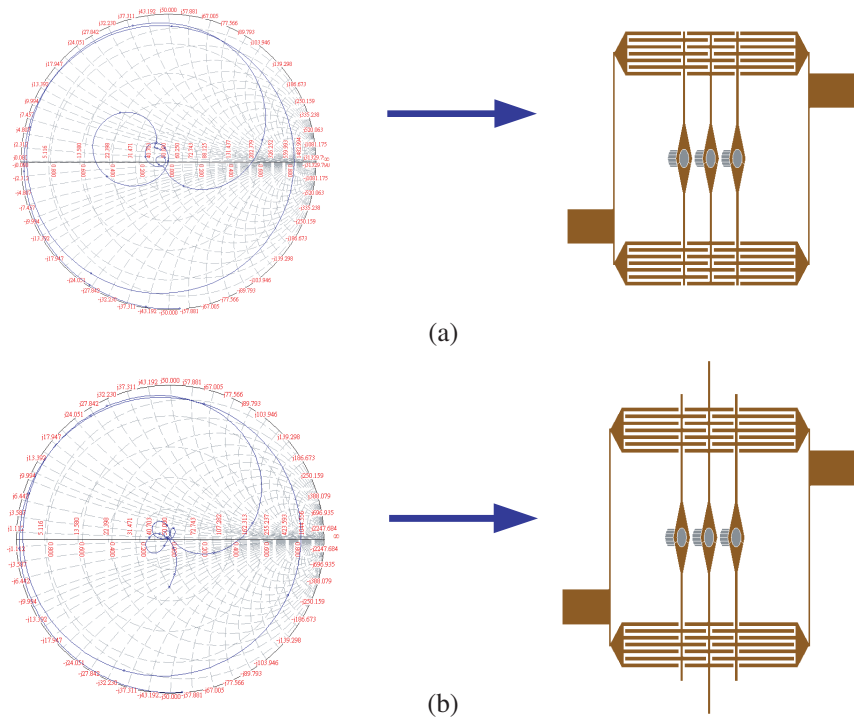of the open stub structure.

(a)

(b)

Figure 7. The performance verification using the Smith Chart. (a) Without open stubs. (b) With open stubs structure.

3. SIMULATION AND MEASUREMENT RESULTS

To demonstrate the applications of the studies in the previous sections, a novel three cells bandpass filter using CRLH TL based on the $0°$ feeding structure is proposed in Fig. 8. They are designed using the simulation solver IE3D and fabricated on an RT/duroid 4003 substrate with a thickness $h = 20$ mil and a relative dielectric constant $\varepsilon_r = 3.38$. The dimensions of the proposed filter are specified as follows: $L_1 = 4.15$ mm, $L_2 = 1.7$ mm, $W_s = 0.2$ mm, $W_i = 0.15$ mm, $d = 0.1$ mm, $v = 0.7$ mm, and the scheme size is 14.8 mm $\times 12.84$ mm. The S-parameter simulation and measurement results for this designed filter are shown in Fig. 9. The passband with center frequency of 4.2 GHz has insertion loss of less than 1.1 dB and return loss of greater than 25 dB. The 3-dB bandwidth is 1.8 GHz from 3.3 GHz to 5.1 GHz. Compared to the simulated results, the measured bandwidth agrees fairly well with the simulated bandwidth. In addition, the proposed

bandpass filter can generate transmission zeros and provide a better
cutoff rate outside the passband. Two transmission zeros are located at
2.95 GHz and 6.18 GHz with attenuations of −44.1 dB and −37.3 dB,
respectively. Also, a wide rejection band ranged from 5.4 to 9 GHz
is obtained. Figs. 10(a) and (b) show the IE3D-simulated current
distribution at 2.95 and 6.18 GHz. It is observed that the current flows
from the series interdigital capacitors to the shunt short-circuited stub
inductors. For wideband application, the investigation of the flat group
delay is important and required. The simulated and measured group
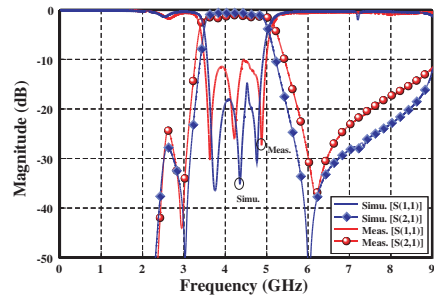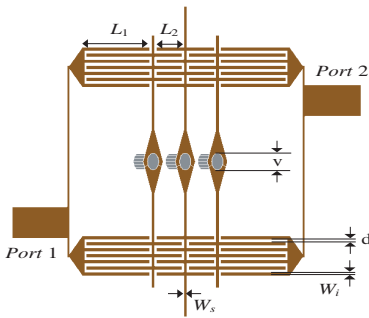delays are shown in Fig. 11. Fig. 12 shows the photograph of this
structure.

Figure 8. The novel CRLH scheme based on the 0° feed structure.
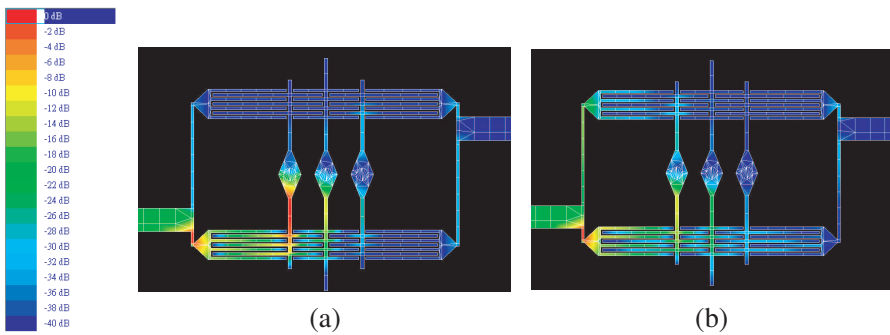

Figure 9. Simulation and measurement results.

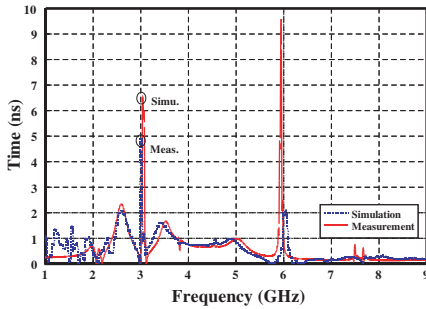**Figure 10.** The current distribution at (a) 2.95 GHz and (b) 6.18 GHz.

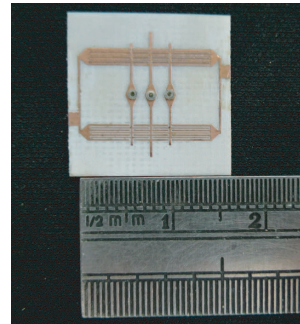**Figure 11.** Group delay of the proposed dual-band filter.

Figure 12. Structure photograph (scheme size = 14.8 × 12.84 mm²).

4. CONCLUSION

This paper presents a novel compact CRLH microstrip bandpass filter. To realize wide rejection band and provide more compact size, the circuit is designed to be unbalanced. A tunable gap between left handed and right handed modes in the $\beta - \omega$ diagram can control out of band performance. With careful design, a bandpass filter with wide rejection band can be achieved. By adding 0° feeding structures, the frequency selectivity of the filter is much improved. It has been shown that the proposed microstrip bandpass filter can be designed and fabricated with 1.1-dB insertion loss at the center frequency of 4.2 GHz and about 42.86% 3-dB bandwidth Two transmission zeros are located at 2.95 GHz and 6.18 GHz with -44.1 dB and -37.3 dB, respectively. Also, a wide rejection band from 5.4 to 9 GHz is obtained. Compared with the reported documents, it has the advantages of low insertion loss, enhancing the interference immunity, and compact size. Numerical simulations using IE3D show good agreements with experiments.

ACKNOWLEDGMENT

REFERENCES

1. Veselago, V., "The electrodynamics of substances with simultaneously negative values of ε and μ," *Soviet Physics Uspekhi*, Vol. 10, No. 4, 509–514, Jan.–Feb. 1968.

2. Simovski, C. R., P. A. Belov, and H. Sailing, "Backward wave region and negative material parameters of a structure formed by lattices of wires and split-ring resonators," *IEEE Trans. Antennas Propagat.*, Vol. 51, 2582–2591, Oct. 2003.

3. Ziolkowski, R. W. and A. D. Kipple, "Application of double negative materials to increase the power radiated by electrically small antennas," *IEEE Trans. Antennas Propagat.*, Vol. 51, 2626–2640, Oct. 2003.

4. Kim, H., A. B. Kozyrev, A. Karbassi, and D. W. Van derWeide, "Linear tunable phase shifter using a left-handed transmission line," *IEEE Microw. Wireless Compon. Lett.*, Vol. 15, No. 5, 366–368, May 2005.

5. Mao, S.-G., M.-S. Wu, Y.-Z. Chueh, and C. H. Chen, "Modeling of symmetric composite right/left-handed coplanar waveguides with applications to compact bandpass filters," *IEEE Trans. Microw. Theory Tech.*, Vol. 53, No. 11, 3460–3466, Nov. 2005.

6. Zhu, L., V. K. Devabhaktuni, and C. Wang, "CAD of left-handed transmission line bandpass filters," *PIERS Online*, Vol. 3, No. 1, 77–82, 2007.

7. Li, C., K. Y. Liu, and Fang Li, "Analysis of composite right/left-handed coplanar waveguide zeroth-order resonators with application to a band-pass filter," *PIERS Online*, Vol. 3, No. 5, 599–602, 2007.

8. Hirota, A., Y. Tahara, and N. Yoneda, "A compact forward coupler using coupled composite right/left-handed transmission lines," *IEEE Trans. Microw. Theory Tech.*, Vol. 57, No. 12, 3127–3133, Dec. 2009.

9. Sanada, A., C. Caloz, and T. Itoh, "Characteristics of the composite right/left-handed transmission lines," *IEEE Microw. Wireless Compon. Lett.*, Vol. 14, No. 2, 68–70, Feb. 2004.

10. Tsai, C.-M., S.-Y. Lee, and C.-C. Tsai, "Performance of a planar filter using a zero-degree feed structure," *IEEE Trans. Microwave Theory and Tech.*, 2362–2367, Oct. 2002.

11. Lim, S., C. Caloz, and T. Itoh, "Metamaterial-based electronically controlled transmission line structure as a novel leaky-wave antenna with tunable radiation angle and beamwidth," *IEEE Trans. Microwave Theory Tech.*, Vol. 53, No. 1, 161–173, Jan. 2005.

12. Caloz, C., A. Sanada, and T. Itoh, "A novel composite right-/left-handed coupled-line directional coupler with arbitrary coupling level and broad bandwidth," *IEEE Trans. Microw. Theory Tech.*, Vol. 52, No. 3, 980–992, Mar. 2004.